

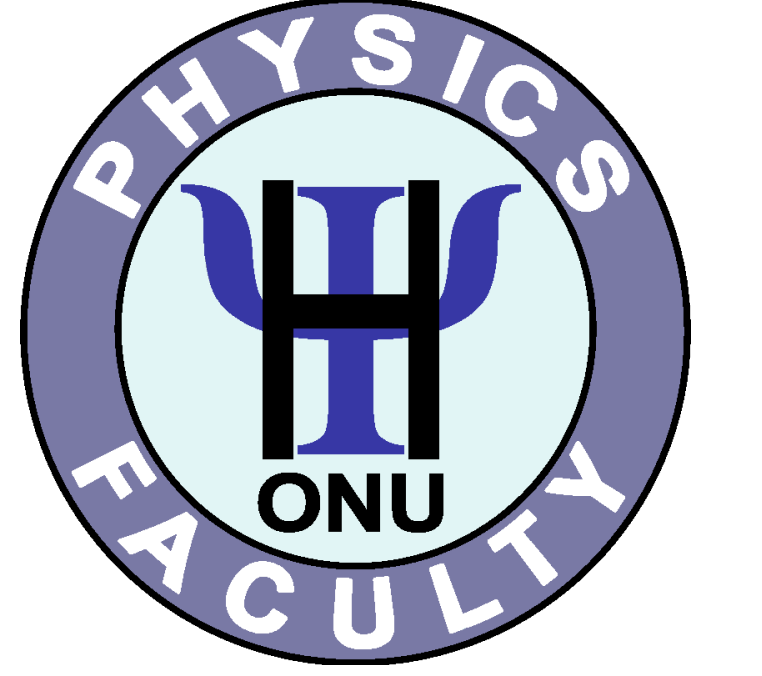
Global isomorphism between the Lennard-Jones fluids and the



Ising model

Vladimir Kulinskii

Odessa I.I. Mechnikov National University,
Department of Theoretical Physics, 2 Dvoryanskaya Str., Odessa 65026, Ukraine
kulinskij@onu.edu.ua



1. Empirical facts

The search of the universal relations which applicable to broad class of substances is of great importance. One of the most known is the principle (theorem) of corresponding states (PCS) which goes back to van der Waals [1]. Well-known the rectilinear diameter law (RDL) [2] for the density as the order parameter of the phase coexistence:

$$n_d = \frac{n_{liq} + n_{gas}}{2n_c} - 1 = A|\tau| + \dots, \quad \tau = \frac{T - T_c}{T_c} \quad (1)$$

is another example. Although the relation (1) is also approximate it is observed for a wide variety of fluids in a surprisingly broad temperature interval beyond the critical region. Another typical phenomenological Batchinsky law was derived from the van der Waals equation [3]:

$$p = \frac{nT}{1 - nb} - an^2$$

It states that the curve defined by the equation $Z = 1$, where $Z = \frac{p}{nT}$ is the compressibility factor, is a straight line which can be described by simple equation on (n, T) -plane:

$$\frac{n}{n_B} + \frac{T}{T_B} = 1. \quad (2)$$

where $T_B = a/b$ is the Boyle point and $n_B = 1/b$. In work of Ben-Amotz and Herschbach [4] the line $Z = 1$ is called by the Zeno-line (ZL). They also noted the striking correlation between two remarkable linearities (1) and (2).

These findings have been further developed in works of Apfelbaum & Vrob'ev [5]. These authors formulated the conception of the "Triangle of Liquid-Gas States" [5]. We show that the facts (1) and (2) can be naturally explained within the conception of the global isomorphism between the Lattice Gas (LG) or equivalently the Ising model given by the Hamiltonian:

$$H = -J \sum_{\langle ij \rangle} n_i n_j - \mu \sum_i n_i, \quad n_i = 0, 1 \quad (3)$$

and simple fluids.

2. Liquid-vapor binodal as the image of the binodal of the lattice model

It is easy to see that linear laws (1) and (2) are fulfilled trivially in the case of the Lattice Gas (LG) model or equivalently the Ising model. Indeed, the rectilinear diameter law for the LG is fulfilled due to the symmetry of the Hamiltonian (3) with respect to the line $x = 1/2$.

The analog of the Zeno-line for the LG can be defined too. In this case it is the line $x = 1$ where the "holes" are absent. It is clear that if $x = 1$ then the perfect configurational order takes place and the site-site correlation function for (3) vanishes:

$$\langle \langle q_i q_j \rangle \rangle = \langle q_i q_j \rangle - \langle q_i \rangle \langle q_j \rangle = 0.$$

Thus the line $x = 1$ plays the role of the Zeno-line on the $x-t$ phase diagram of the LG. Due to simple structure of the LG Hamiltonian (3) and explicit symmetries there are degenerate elements of the phase diagram. The critical isochore $x_c = 1/2$ coincides with the diameter. The Zeno-line is the tangent to the binodal in this case expands up into the region $t \rightarrow 0$. Thus there is the degeneration of these in the case of the LG. Naturally, that both mentioned degenerations for the linear elements (1) and (2) of the phase diagram disappear for the real fluids. The difference of the diameter and the isochore is nothing but the asymmetry of the binodal. The definition of the tangent linear element

$$\frac{n}{n_*} + \frac{T}{T_*} = 1 \quad (4)$$

relies upon the van der Waals approximation for the given EoS and therefore does not coincide with the Zeno-line. The parameters entering (4) are:

$$T_B^{(vdW)} = \frac{a}{b}. \quad (5)$$

where

$$a = -2\pi \int_{\sigma}^{+\infty} \Phi_{attr}(r) r^2 dr \quad (6)$$

and $\Phi_{attr}(r)$ is the attractive part of the full potential $\Phi(r)$, σ is the effective diameter of the particle so that $b = \frac{2\pi}{3} \sigma^3$,

$$n_* = \frac{T_*}{B_3(T_*)} \frac{dB_2}{dT} \Big|_{T=T_*}. \quad (7)$$

This relation follows from the constraint that the compressibility factor Z changes linearly with the change of the temperature T along the linear element (4).

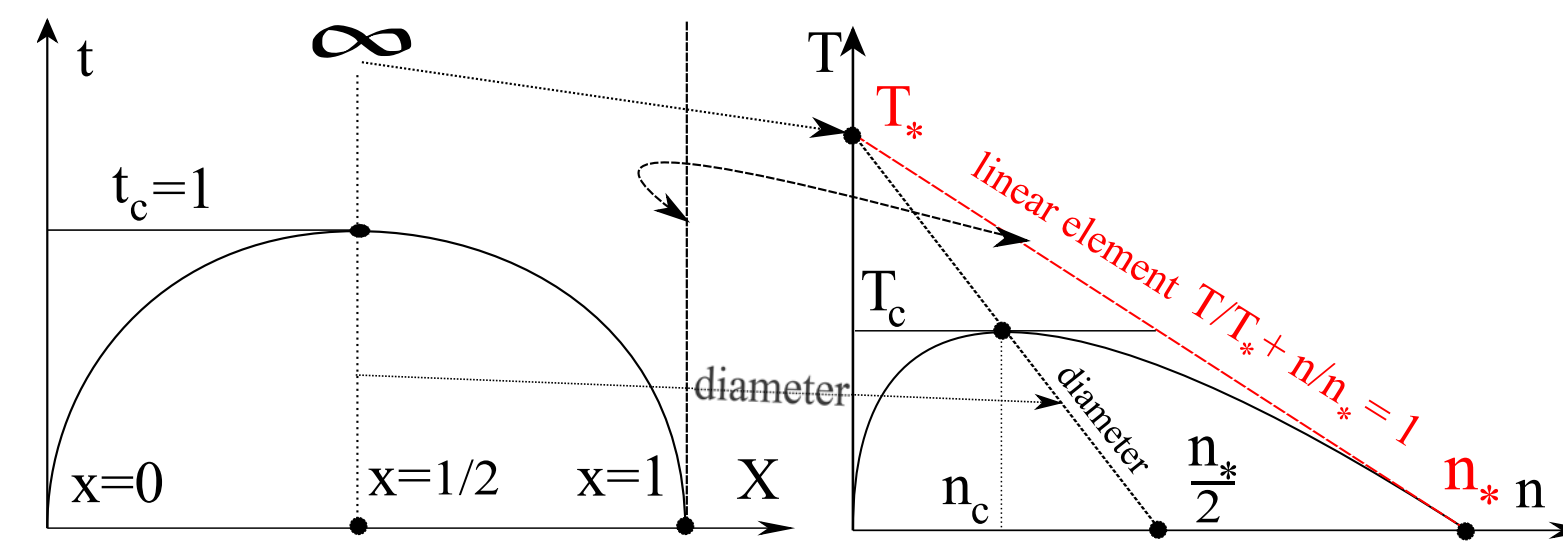


Figure 1: The geometrical correspondence between the elements of the thermodynamic phase diagram.

Because of linearity of the characteristic elements (1) and (4) the following transformation:

$$n = n_* \frac{x}{1 + zt}, \quad T = T_* \frac{z}{1 + zt}, \quad (8)$$

maps the phase diagrams of the Lattice Gas and the continuum fluid. Obviously z is as following:

$$z = \frac{T_c}{T_* - T_c}. \quad (9)$$

(8) provides the mapping between the binodals of the LG (Ising model) and Lennard-Jones (LJ) fluid with the potential

$$\Phi(r) = 4U_0 \left(-\left(\frac{\sigma}{r}\right)^6 + \left(\frac{\sigma}{r}\right)^{12} \right). \quad (10)$$

In accordance with (16) (see below), $z = 1/3$ for 2D LJ fluid and $z = 1/2$ for 3D case respectively. For 2D case the known exact solution for 2D Ising model is:

$$x = 1/2 \pm f(t)^{1/8}, \quad f(t) = 1 - \frac{1}{\sinh^4(2J/t)}. \quad (11)$$

Substituting (11) into (8) the parametric representation for the binodal of LJ fluid is obtained and can be compared with the known numerical simulation results (see Fig. 2). Note that the values of the parameters T_* and n_* obtained by fitting are very close to that following from the consideration above $T_* \approx T_B^{vdW} = 2$ and $n_* \approx 0.91$ (see also [6]). The locus of the CP obtained is in good correspondence with the results of [7].

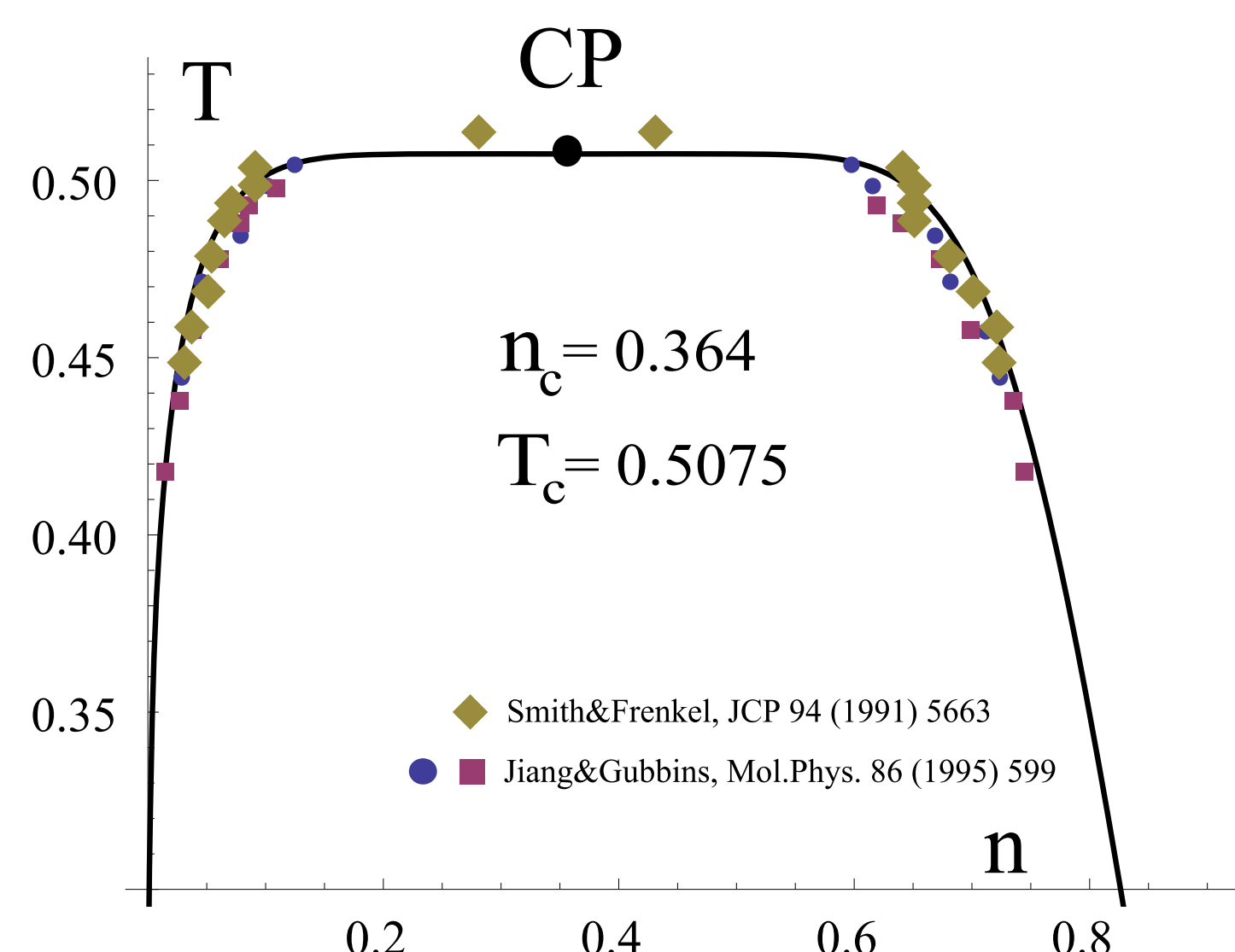


Figure 2: Fitting the binodal of two dimensional LJ fluid (8) with $z = 1/3$, $T_* = 2.03$ and $n_* = 0.971$ to the results of the simulations [8, 7]. Also the corresponding locus of the CP is shown.

The empirical EoS for 3D Ising binodal

$$x = \frac{1}{2} \left(1 \pm \tau^\beta \left(b_0 + a_1 \tau + a_{\Delta_1} \tau^{\Delta_1} \right) \right), \quad \tau = 1 - t, \quad (12)$$

where $\beta = 0.326941$, $\Delta_1 = 0.50842$, $b_0 = 1.6919$, $a_1 = -0.42572366$, $a_{\Delta_1} = -0.34357731$ was obtained in [9]. This expression represents the data in the region $0.0005 < \tau < 0.26$. In Fig. 3 the result of mapping (8) onto $n - T$ plane is shown. The experimental data are shown by "o".

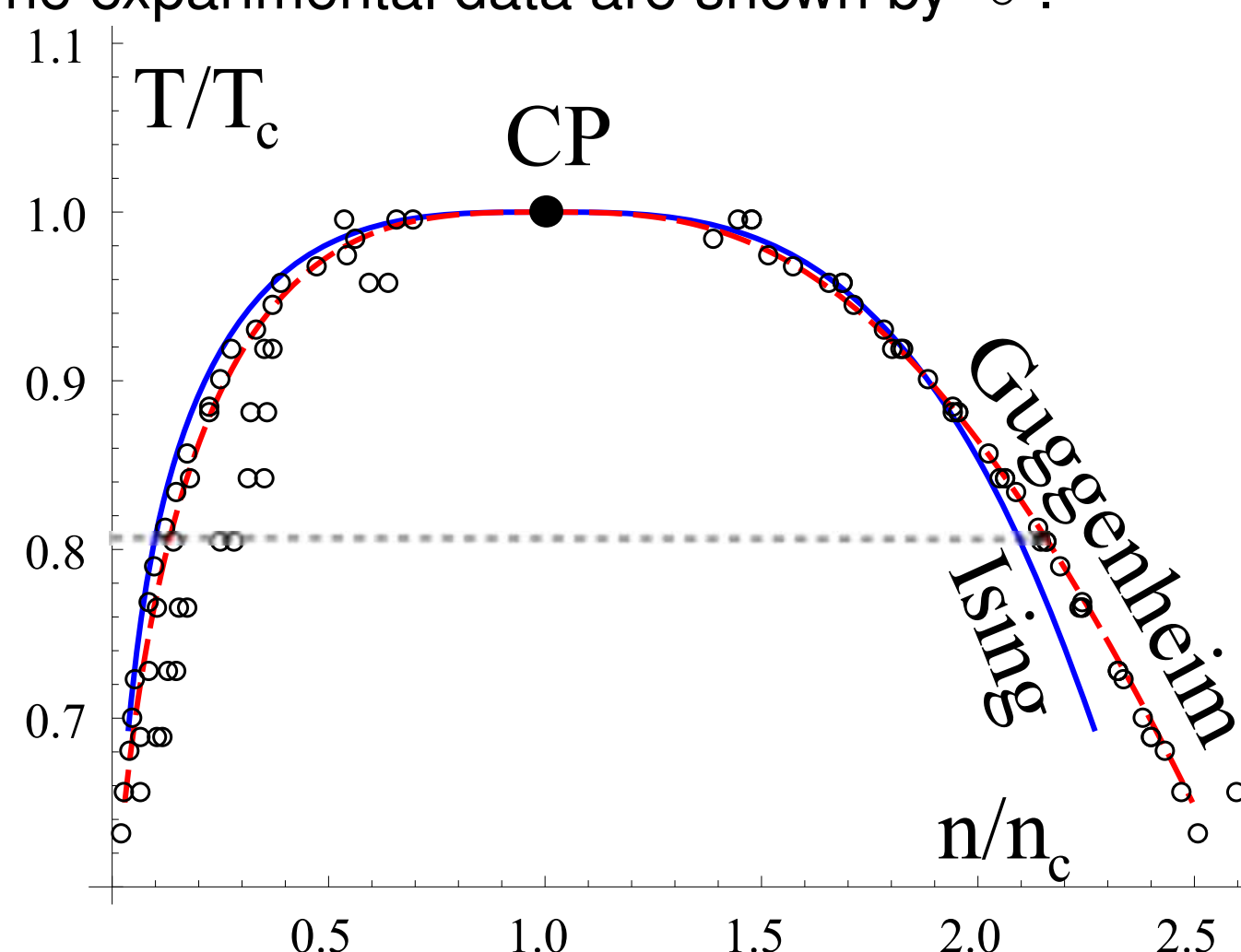


Figure 3: Binodal for 3D LJ fluid (blue line) obtained from the mapping of the empirical EoS of the 3D Ising model after transformation (8) with $z = 1/2$, $T_* = T_B^{(vdW)} = 4$ and $n_* = 0.94$.

3. The locus of the critical point for the Lennard-Jones fluid

In (8) the critical parameters of the LG is $x_c = 1/2$, $t_c = 1$. The coordinates of the CP for the fluid are:

$$n_c = \frac{n_*}{2(1+z)}, \quad T_c = T_* \frac{z}{1+z}. \quad (13)$$

In addition to (9) the parameter z can be connected with the properties of the attractive potential. The scaling relation:

$$-\frac{d \ln(T_c/T_*)}{d \ln(n_c/n_*)} = \frac{1}{z}, \quad (14)$$

directly follows from (13). This leads to:

$$\frac{d \ln \left(\left| \Phi_{att}(n_c^{-1/d}) \right| / T_* \right)}{d \ln(n_c/n_*)} = \frac{1}{z} \quad (15)$$

If the attractive part of the potential has the power-like asymptotic $\Phi_{att}(r) \propto r^{-m}$, $m > d$ then

$$z = d/m. \quad (16)$$

E.g. for three dimensional Lennard-Jones potential $z = 1/2$.

LJ "6-12" fluid	2D	3D	4D	5D
T_c	0.5	1.333	3.2	9.08
$T_c^{(num)}$, [10]	0.515	1.312	3.404	8.8 (?)
n_c	0.353	0.322	0.404	0.693
$n_c^{(num)}$, [10]	0.355	0.316	0.34	-

Table 1: The comparison of the estimates (13) with the results of numerical simulations [10]. The value $T_c^{5D} \approx 8.8$ of the critical temperature for 5D case was obtained in [10] by simple extrapolation of the results for lower dimensions.

The approach can be applied to the Mie-potentials:

$$\Phi(r; m, q) = \varepsilon \frac{m}{q - m} \left(\frac{q}{m} \right)^{q/(q-m)} \left(\left(\frac{\sigma}{r} \right)^q - \left(\frac{\sigma}{r} \right)^m \right), \quad (17)$$

Further we pay special attention to the case $m = 6$, for which the extensive numerical results are available [11, 12, 13]. Using (13) it is possible to relate the critical temperatures for $\Phi(r; 6, q)$ with different q [14]:

$$T_*(q) = 2 \sqrt{\frac{6}{q-6}} \left(\frac{q}{6} \right)^{\frac{q}{2(q-6)}} \Rightarrow T_c(q) = \frac{2}{3} \sqrt{\frac{6}{q-6}} \left(\frac{q}{6} \right)^{\frac{q}{2(q-6)}}. \quad (18)$$

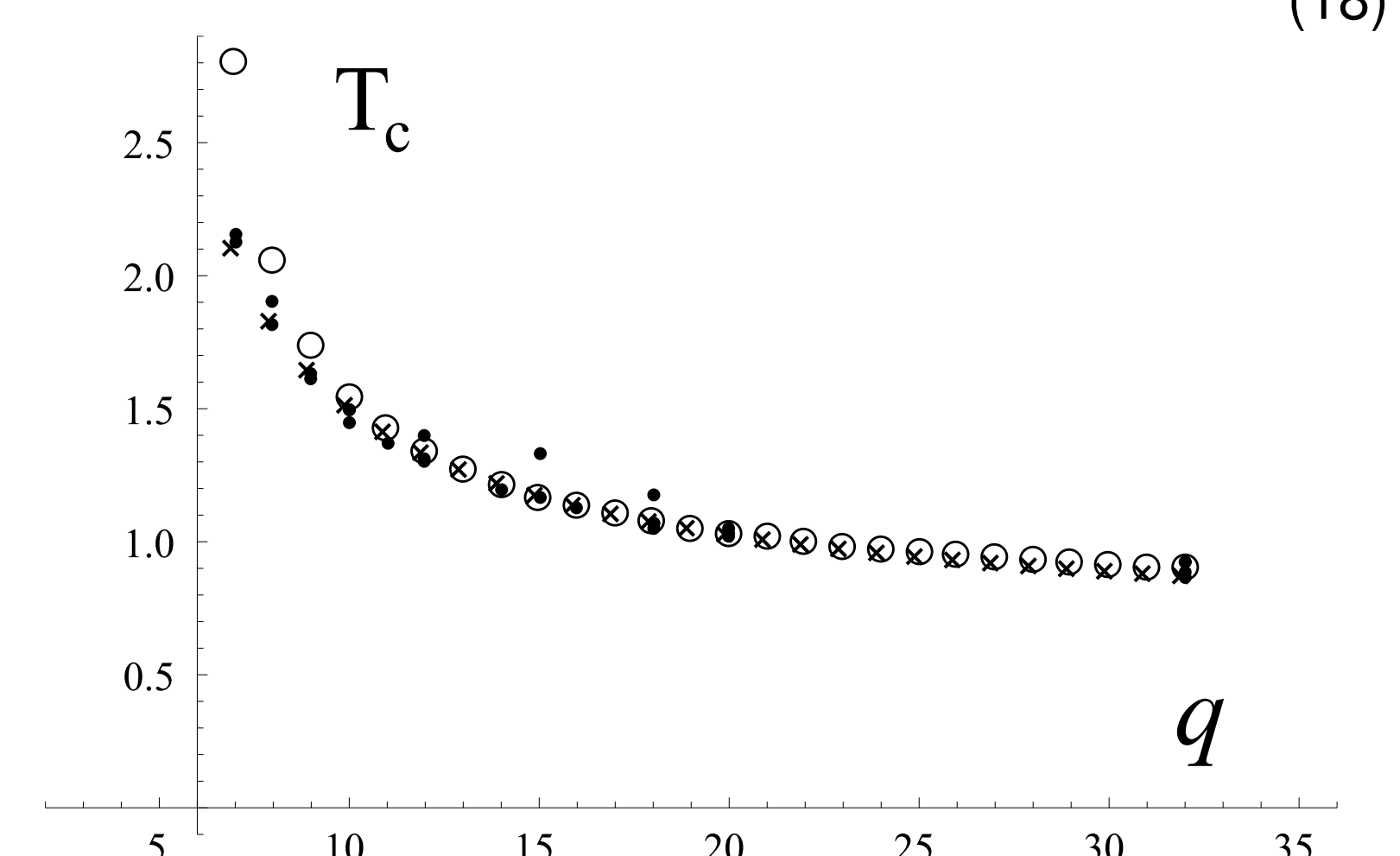


Figure 4: Critical temperature T_c of Mie(6, q)-fluid: theory (open) and the numerical data (filled) [11, 15, 16].

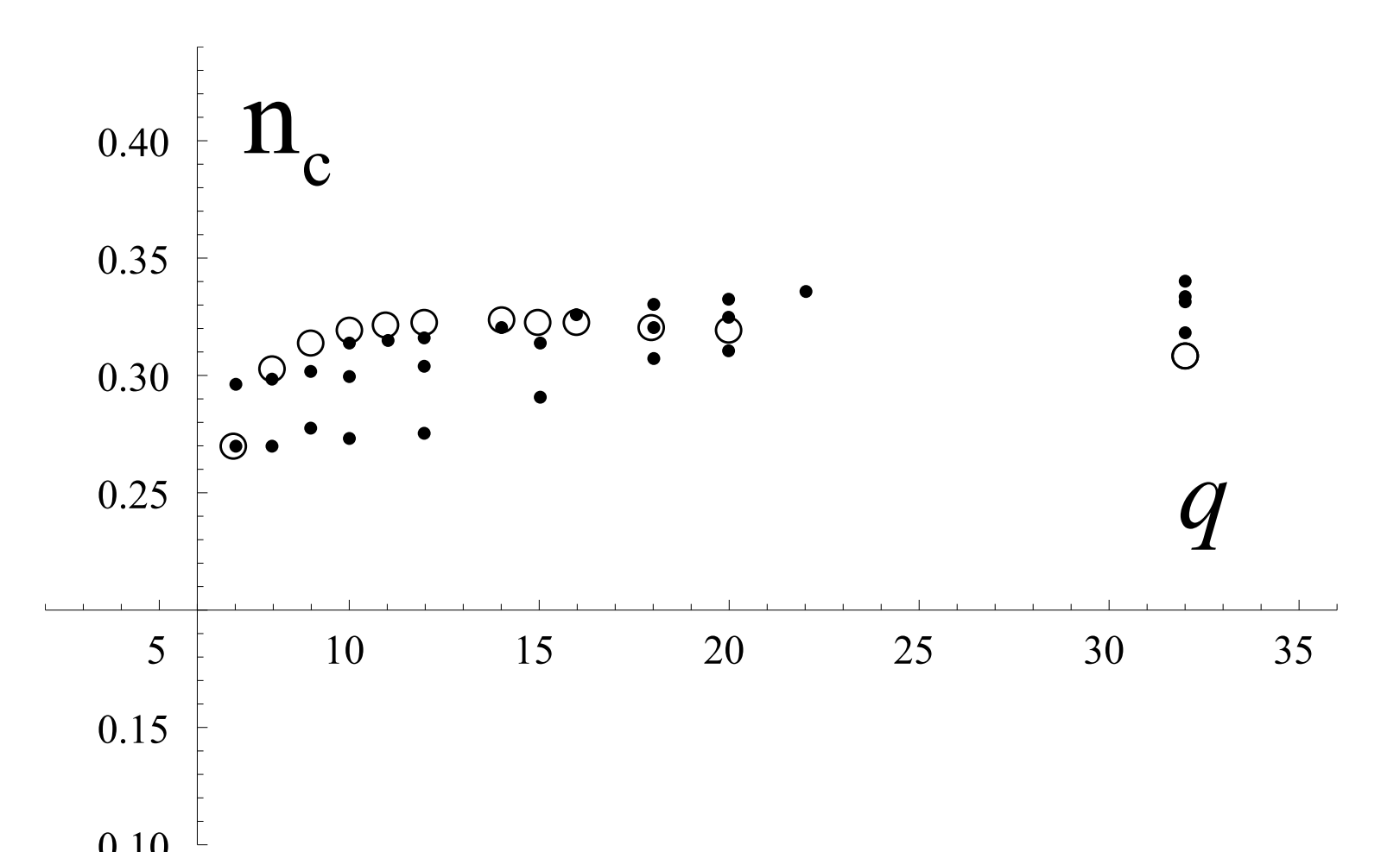


Figure 5: Critical density n_c of Mie(6, q)-fluid: theory (open circles) and the numerical data (points) [11, 15, 16].

The results for the Sutherland potential can be obtained from (18) by taking the limit $q \rightarrow \infty$. The results are shown in Tables 2 and Figs. 4, 5.

m	n_c	$n_c^{(num)}$	T_c	$T_c^{(VL)}$	$T_c^{(num)}$
3.1	0.254	0.247	14.75	8.14	11.45
4	0.286	0.299	1.286	1.307	1.37
6	0.333	0.376	0.667	0.574	0.597

Table 2: The results for the Sutherland potential ($Mie(6, q)$, $q = \infty$).

The same procedure can be applied to the Buckingham potential:

$$\Phi_B(x; a) = \begin{cases} \infty, & x \leq r_0/r_m, \\ \frac{\varepsilon}{1-6/a} \left(\frac{6}{a} \exp(a(1-x)) - \frac{1}{x^6} \right), & x > r_0/r_m, \end{cases} \quad (19)$$

where $x = r/r_m$ and r_0 determines the hardcore cut-off and is defined by the point of maximum of Φ_B . The distance r_m is the point where Φ_B reaches minimum $\Phi_B(r_0) = -\varepsilon$. Also the distance where Φ_B crosses zero we denote σ . It depends on the parameter a and clearly $r_0 < \sigma < r_m$. Note that for the Buckingham potential it is handy to make the distance dimensionless in units of r_m and use the corresponding dimensionless density $n r_m^3$. Comparing (17) for $m = 6$ and (19) we see that the corresponding change of scale is needed. It is easy to find that at $a \approx 12.8$ the attractive part of the Buckingham potential equals to that of the standard LJ 6-12 potential $\Phi(r; 6, 12)$ and therefore for such potential $T_c = T_B^{(vdW)}/3$. So we choose this case as the reference point. The analog of (18) is:

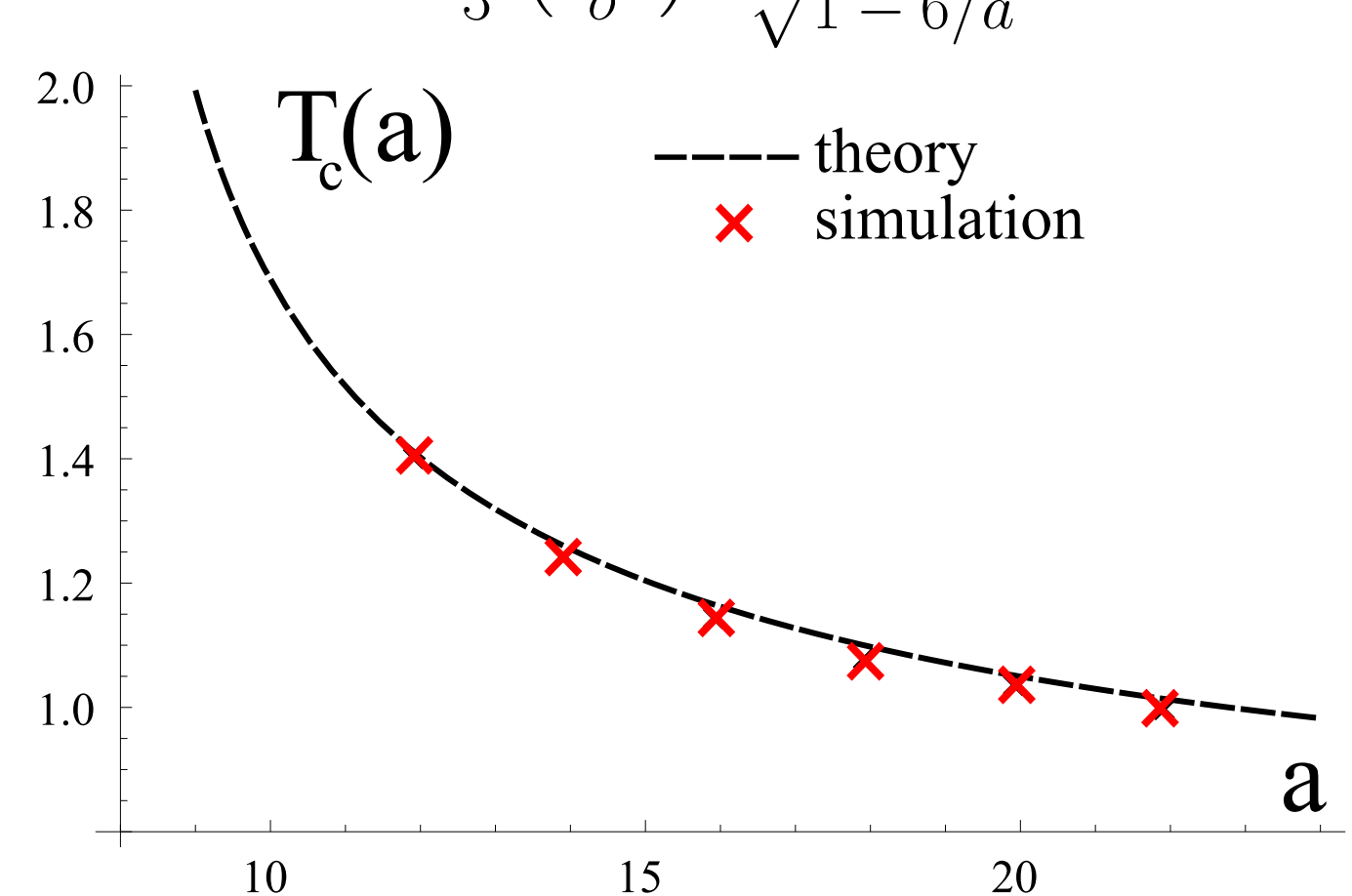
$$T_c(a) = \frac{2}{3} \left(\frac{r_m}{\sigma} \right)^3 \frac{1}{\sqrt{1-6/a}}. \quad (20)$$


Figure 6: Critical temperature T_c of Buckingham potential: theory (dashed) and the numerical data from [17].

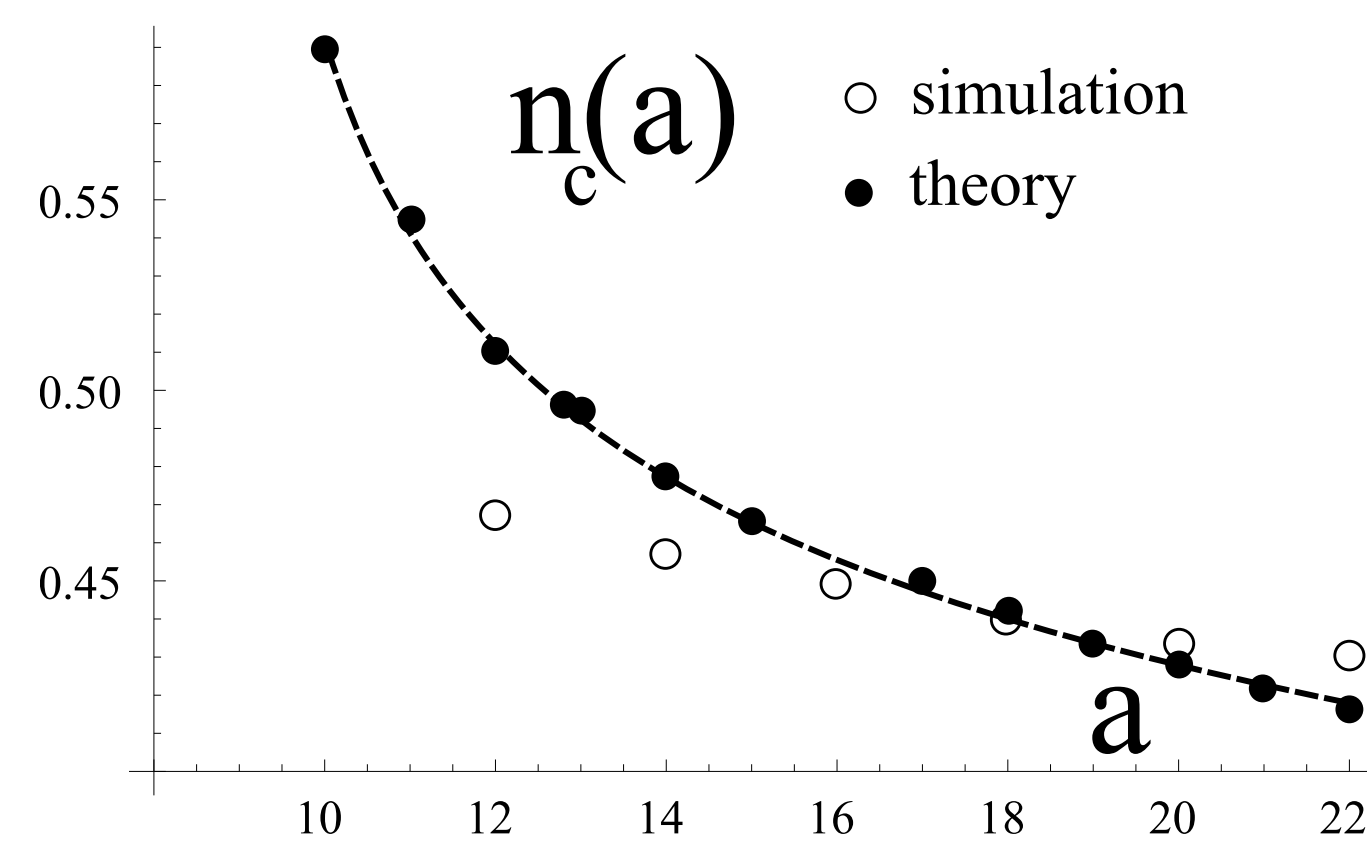


Figure 7: Critical density n_c of Buckingham potential. The numerical data (open) from [17]. The dashed line is the interpolation of the calculated values of n_c .

The comparison of the results and available numerical data

for the Buckingham potential is given in Figs. 6,7.

References

- [1] Johannes Diderik van der Waals. *De Constitutiet van den Gas - En Floeistoestand*. PhD thesis, Leiden University, Leiden, 1873.
- [2] L. Cailletet and E.C. Mathias. *Comptes rendus hebdomadaires des séances de l'Académie des Sciences*, 102:1202, 1886.
- [3] A. Batschinski. Abhandlungen über Zustandgleichung; abh. i: Der orthometrische Zustand;. *Ann. Phys.*, 324:307–309, 1906.
- [4] Dor Ben-Amotz and Dudley R. Herschbach. Correlation of Zeno ($Z=1$) line for supercritical fluids with vapor-liquid rectilinear diameter. *Israel Journal of Chemistry*, 30:59–68, 1990.
- [5] E. M. Apfelbaum, V. S. Vorob'ev, and G. A. Martynov. Triangle of Liquid-Gas states. *Journal of Physical Chemistry B*, 110:8474, 2006.
- [6] V. L. Kulinskii. Global isomorphism between the Lennard-Jones fluids and the ising model. *The Journal of Chemical Physics*, 133(3):034121, 2010.
- [7] Shaoyi Jiang and Keith E. Gubbins. Vapour-liquid equilibria in two-dimensional lennard-jones fluids: unperturbed and substrate-mediated films. *Molecular Physics*, 86(4):599–612, 1995.
- [8] Rajiv R. Singh, Kenneth S. Pitzer, Juan J. de Pablo, and John M. Prausnitz. Monte Carlo simulation of phase equilibria for the two-dimensional Lennard-Jones fluid in the Gibbs ensemble. *The Journal of Chemical Physics*, 92(9):5463–5466, 1990.
- [9] A. L. Talapov and H. W. J. Blote. The magnetization of the 3d Ising model. *Journal of Physics A: Mathematical and General*, 29(17):5727–5733, 1996.
- [10] M. Hloucha and S. I. Sandler. Phase diagram of the four-dimensional Lennard-Jones fluid. *The Journal of Chemical Physics*, 111(17):8043–8047, 1999.
- [11] Hisashi Okumura and Fumiko Yonezawa. Liquid-vapor coexistence curves of several interatomic model potentials. *The Journal of Chemical Physics*, 113(20):9162–9168, 2000.
- [12] Hisashi Okumura and Fumiko Yonezawa. Molecular dynamics study of liquid-vapor coexistence curves and supercritical fluids. *Physica B: Condensed Matter*, 296(1-3):180 – 183, 2001.
- [13] Pedro Orea, Yuri Reyes-Mercado, and Yurko Duda. Some universal trends of the mie(n,m) fluid thermodynamics. *Physics Letters A*, 372(47):7024 – 7027, 2008.
- [14] V. L. Kulinskii. Simple geometrical interpretation of the linear character for the Zeno-line and the rectilinear diameter. *Journal of Physical Chemistry B*, 114(8):2852–2855, 2010.
- [15] Athanassios Z. Panagiotopoulos. On the equivalence of continuum and lattice models for fluids. *The Journal of Chemical Physics*, 112(16):7132–7137, 2000.
- [16] I. Charpentier and N. Jakse. Phase diagram of complex fluids using an efficient integral equation method. *The Journal of Chemical Physics*, 123(20):204910, 2005.
- [17] Jeffrey R. Errington and Athanassios Z. Panagiotopoulos. Phase equilibria of the modified buckingham exponential-6 potential from hamiltonian scaling grand canonical Monte Carlo. *The Journal of Chemical Physics*, 109(3):1093–1100, 1998.